frontiers | Frontiers in Earth Science

TYPE Original Research
PUBLISHED 18 June 2024
DOI 10.3389/feart.2024.1398474

OPEN ACCESS

EDITED BY
Haijun Song,
China University of Geosciences Wuhan, China

REVIEWED BY
Li Tian,
China University of Geosciences Wuhan, China
Jingxin Jiang,
Nanjing University, China

*CORRESPONDENCE
Dangpeng Xi,
xdp1121@163.com

RECEIVED 10 March 2024
ACCEPTED 05 April 2024
PUBLISHED 18 June 2024

CITATION
Fang S, Xi D, Sun Q, Li D, Yang Z, Liu D, Wu Y, Jiang T and Wan X (2024), The bivalve-bearing carbonate platform on the east Tethys during the middle Eocene and its response to the Tethys transgression. *Front. Earth Sci.* 12:1398474. doi: 10.3389/feart.2024.1398474

The bivalve-bearing carbonate platform on the east Tethys during the middle Eocene and its response to the Tethys transgression

Shaobo Fang[1], Dangpeng Xi[1]*, Qi Sun[1], Dalei Li[2], Zhangzhang Yang[2], Dan Liu[1], Yuyang Wu[1], Tian Jiang[1] and Xiaoqiao Wan[1]

[1]State Key Laboratory of Biogeology and Environmental Geology, China University of Geosciences, Beijing, China, [2]Shaanxi Geology and Mining First Geological Team Co., Ltd, Ankang, Shaanxi, China

The Eocene was a typical greenhouse climate period in the history of the Earth, with a high global sea level and extensive carbonate deposits developed in Tethys. During the Eocene, a carbonate platform was deposited in the western Tarim Basin, which belongs to the easternmost Tethys. However, the details of this carbonate platform and its complications for paleoecology and paleoclimate are still unclear. This research focuses on the bivalve-bearing carbonates of the Kalataer Formation in the western Tarim Basin, and detailed analyses of microfacies, biostratigraphy, paleoecology, and sea-level change were carried out. The bivalves of the Kalataer Formation are dominated by the *Ostrea* (*Turkostrea*) *strictiplicata*, *Ostrea* (*Turkostrea*) *cizancourti, Ostrea* (*Turkostrea*) *strictiplicata*, *Ostrea* (*Turkostrea*) *strictiplicata,* and *Sokolowia buhsii*, and the age is middle Lutetian of the Eocene. The biota of the Kalataer Formation mainly lives in open shallow sea environments, with medium to low energy and rich nutrients and oxygen, representing a typical shallow marine ecosystem of the carbonate platform. Microfacies and paleoecology indicate a large marine transgression event occurred in the western Tarim Basin during the middle Eocene.

KEYWORDS

Tarim Basin, carbonate platform, bivalves, Eocene, marine transgression, TETHYS

1 Introduction

The Tarim Basin is the largest Mesozoic–Cenozoic sedimentary basin located between the west Kunlun Mountain and the Tianshan Mountains, representing the easternmost branch of the Paratethys Sea (Hao et al., 1982; Mao and Norris, 1988; Zhou and Chen, 1992; Bosboom et al., 2011; Cao et al., 2018; Jiang et al., 2023). The Paleogene sediments of the western Tarim Basin remnants of the easternmost extent of a large epicontinental sea (Tang et al., 1992; Bosboom et al., 2011; Bosboom et al., 2014a; Xi et al., 2016). As the global rise in sea level and tectonic forcing, the Paratethys covered the southwest Tarim Basin during Late Cretaceous to Paleogene (Hao et al., 1982; Tang et al., 1992; Bosboom et al., 2011; Sun and Jiang, 2013; Wang et al., 2014; Xi et al., 2016; 2020).

The Eocene Kalataer Formation, which is widely exposed in the western Tarim Basin, represented the fourth marine transgression from Cretaceous to Paleongene and yielded abundant bivalve fossils (Figure 2B). Though Cretaceous to Paleongene Stratigraphy and sea-level history of the Tarim Basin have been studied in detail (Hao et al., 1982; 2001; Hao and Zeng, 1984; Mao and Norris, 1988; Tang et al., 1989; Guo, 1990; 1991; 1995; Zhong, 1992; Jiang et al., 1995; Lan and Wei, 1995; Yang et al., 1995; Lan, 1997; Bosboom et al., 2011; Sun and Jiang, 2013; Wang et al., 2014; Jiang et al., 2018; Xi et al., 2020; Wang et al., 2022; 2023; Jiang et al., 2023), the biostratigraphy, paleoecology, and paleoenvironment of the Eocene Kalataer Formation is still unclear. This study mainly focuses on the Kalataer Formation in the Bashibulake Section in the western Tarim Basin, and a detailed analysis of microfacies, biostratigraphy, paleoecology, and sea-level change was carried out.

2 Geological setting

The western Tarim Basin borders on the piedmont of the western Kunlun Mountain and the southern Tianshan Mountain, and the areal extent of the basin is 560,000 km^2 (Li et al., 2004) (Figure 1A). The western Tarim Basin preserves a continuous stratigraphic sequence spanning the Jurassic to the present (Tang et al., 1989; Hao et al., 2001; Jia et al., 2004). Since the Cenozoic era, a marine sequence below (Aertashi, Qimugen, Gaijitage, Kalataer, Wulagen, and Bashibulake Formations) and a continental sequence above (Keziluoyi, Anjuan, Pakabulake, and Artushi formations) were deposited (Hao et al., 1982; Zhou, 2001; Yin et al., 2002; Xi et al., 2020). The lower part of the Kalataer Formation is dominated by sandy limestone, argillaceous limestone, limestone, silty mudstone, calcareous and argillaceous siltstone, fine-grained sandstone, and gypsum mudstone or gypsum beds; the upper part consists of bioclastic limestone, shelly limestone, and oyster beds. The Kalataer Formation conforms to the underlying and overlying strata with abundant bivalves and a few benthic foraminifers, gastropods, etc. (Zhou, 2001).

3 Materials and methods

The Bashibulake Section (39°48′ N, 74°43′ E) is situated at the western margin of the Tarim Basin (Figure 1B, C). Twenty-eight samples were collected with a sampling interval of 1–5 m (Figure 2).

Samples of 100 g were dispersed in 30% acetic acid for 24 h prior to sieving through a 200-μm sieve. Foraminifers, ostracods, gastropods, and fish teeth were picked from the samples under a low-power binocular microscope.

Microfacies analysis was based on sedimentary structures observed in the field and on fossil assemblages, grain composition, and textures identified in thin sections. Limestones (siliciclastic detritus <10%) and mixed carbonate–siliciclastic rocks (siliciclastic detritus >10%) were described following Dunham (1962) and integrated by Embry and Klovan (1971) and Mount (1985), respectively. The approach to microfacies analysis, including lithological descriptions and environmental interpretations, was adopted from Flügel (2010).

Twenty-eight samples were then prepared for microfacies analysis in thin sections (2.0 cm × 3.0 cm), as illustrated in Figure 4. An optical microscope (Nikon Eclipse E 200) was used to analyze the sedimentological and micropaleontological features of the samples. All related studies were conducted at the micropaleontological laboratory of the China University of Geosciences in Beijing.

4 Microfacies analysis and interpretations

Lithofacies and their paleoenvironmental proxies are recognized based on lithology, physical and biogenic sedimentary structures, and fossils. Eight microfacies (MF) were identified in the Kalataer Formation, and a carbonate-dominated carbonate platform depositional system was recognized. Representative photographs of the field and microfacies are shown in Figures 3, 4.

4.1 Evaporite

4.1.1 MF1 thin-bedded gypsum and gypsiferous argillite (sabkha)

Microfacies 1 (MF1) is distinguished by its grayish-green, stratified gypsum layers possessing a fibrous texture. These layers vary in thickness from several millimeters to centimeters and can extend laterally up to several decimeters (Figures 3A, B). Gypsiferous argillite, dolostone (MF2), or mudstone (MF3) interbeds are common.

Gypsum discontinuously interbedded with argillite and siltstone presenting tuberous, veinal, and lenticular structures suggests deposition in a highly restricted lagoon <2 m-deep or on supratidal lowlands in arid to semi-arid climatic conditions (Purser, 1973).

4.2 Restricted-marine platform

4.2.1 MF2 dolostone (tidal flat, sabkha)

MF2 is brown-yellowish and grayish-greenish homogeneous microsparitic dolostone and dolomitic limestone (Figure 3C), containing sporadic bioclasts or silt-sized terrigenous grains (Figure 4E).

Dolostone, commonly adjacent to bedded gypsum and gypsiferous argillite (MF1) or mudstone (MF3), is formed by intense evaporation from hypersaline brines in a supratidal coastal-sabkha environment (Flügel, 2004).

4.2.2 MF3 mudstone (tidal flat)

MF3 is characterized by massive grayish-green mudstone, lacking carbonate allochems, and containing rare terrigenous grains <100 μm in diameter (Figure 4A).

MF3 corresponds to SMF23 of Flügel (2010). Non-laminated mudstones lacking fossils, commonly found adjacent to bedded gypsum and gypsiferous argillite (MF1) or dolostone

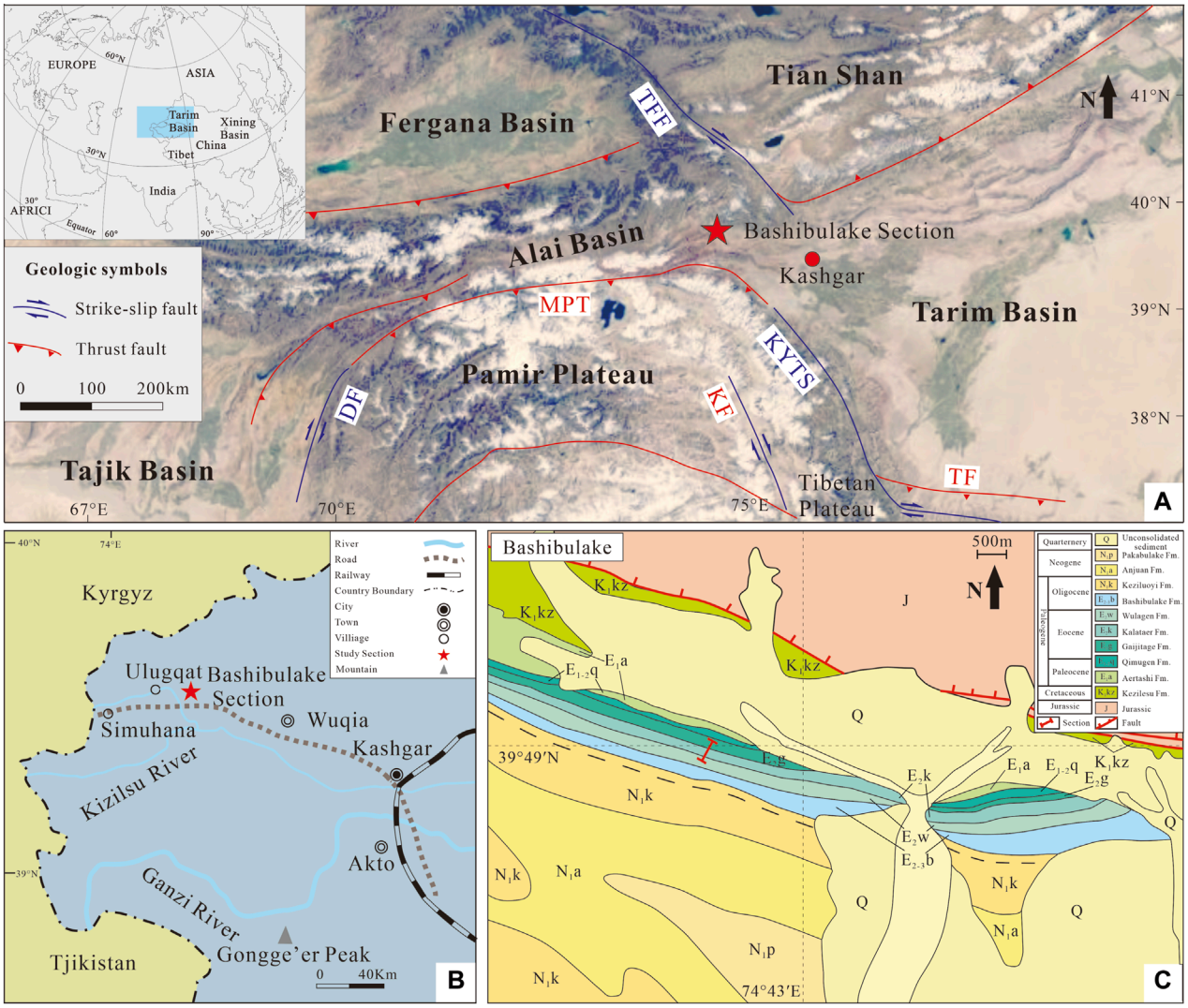

FIGURE 1
(A) Paleogeographic setting of the study area in the early Eocene (after Jiang et al., 2018); **(B)** present location of the Bashibulake Section (after Bosboom, 2011; Cao et al., 2018). **(C)** Geological map of the Bashibulake study areas, modified from the 1:250,000 geological map J43C002002 data (http://www.ngac.org.cn/). Abbreviations: TFF, Talas-Fergana Fault; MPT, Main Pamir Thrust; DF, Darvaz Fault; KYTS, Kashgar-Yecheng transfer fault; KF, Karakoram Fault; TF, Tiklik Fault.

(MF2), suggest a tidal flat environment (Flügel, 2004). Fine-grained windblown terrigenous grains may occur in such environments.

4.2.3 MF4 oolite grainstone (lagoon)

MF4 is gray oolite grainstone (Figure 4B) in the lower to middle parts of the Kalataer Formation. The matrix is dominated by micrite ooids that are 100–400 μm in diameter and commonly show tangential structure and pervasive micritization. Bioclasts and terrigenous grains are lacking. Occasionally, gastropods are present (Figure 4B).

MF4 corresponds to SMF15 of Flügel (2010). Ooid formation needs intermittent agitation of the sea floor to move the grains. According to Figure 4B, the matrix is dominated by micrite, indicating that these oolitic grains were not formed *in situ* but were more likely transported from the oolitic shoal to a relatively stable adjacent water environment, perhaps a lagoon.

4.2.4 MF5 small benthic foraminifer grainstone (lagoon)

MF5 is dominated by gray-greenish small benthic foraminifer grainstone that contains 70%–80% carbonate grains, including various kinds of small benthic foraminifers (5%–15%). The sample contains well-sorted allochems 20–50 μm in diameter, commonly rounded, and showing a micritic envelope (Figure 4F). Locally micritized miliolids and textulariids are common. Gastropods, echinoderms, and calcareous spicules are rare (Figure 4F). Abundant small benthic foraminifers indicate a shallow lagoon environment with water depth not exceeding 10 m (Davies et al., 2002; Ghabeishavi et al., 2010).

10.3389/feart.2024.1398474

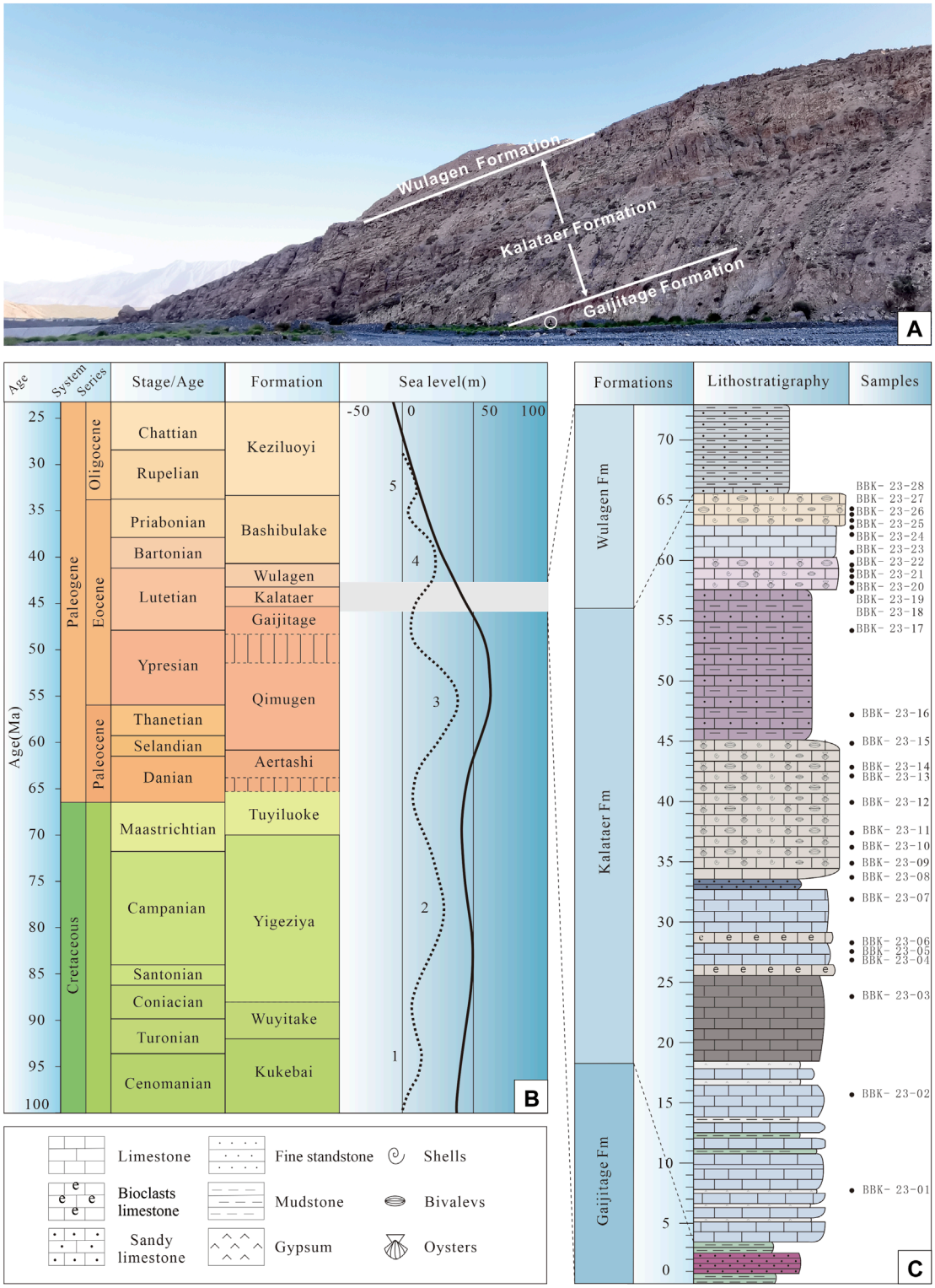

FIGURE 2
(A) Photograph of the study section showing the outcrop of the Kalataer Formation. **(B)** Regional stratigraphy and late Cretaceous to Paleogene sea-level curve for the Tarim Basin (after Bosboom et al., 2014a; Xi et al., 2020). **(C)** Lithological column of the Kalataer Formation with sample distribution in the Bashibulake Section.

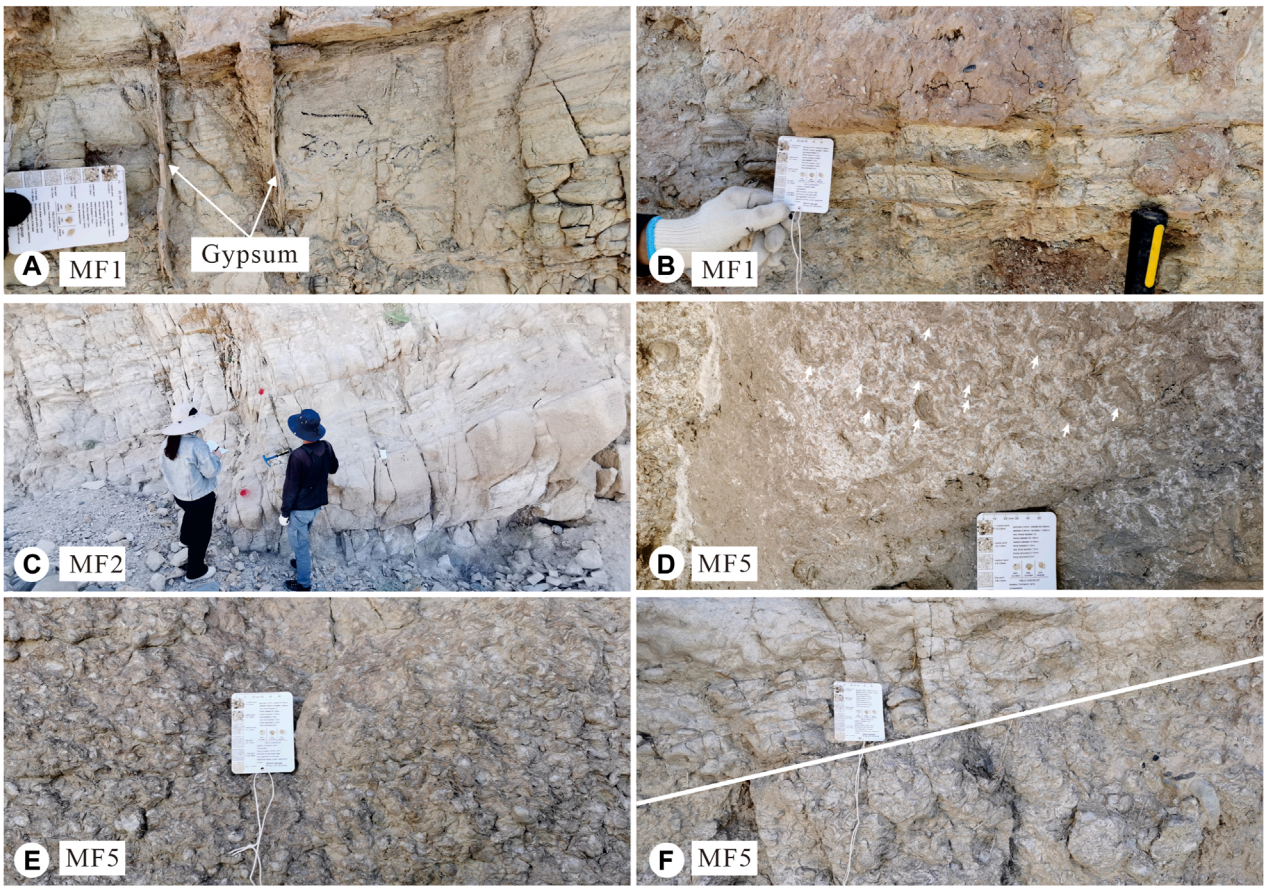

FIGURE 3
(A, B) Gypsiferous argillite from the lower part of the Kalataer Formation; **(C)** laminated dolomite from the lower part of the Kalataer Formation; **(D–F)** oyster shoals from the middle-upper part of the Kalataer Formation.

4.2.5 MF6 bioclastic grainstone

MF6 is dominated by purple-red and grayish-green bioclastic grainstone with well-sorted allochems 100–250 μm in diameter, commonly rounded, and showing a micritic envelope (Figure 4G). Bioclasts include bivalves, bryozoans, benthic foraminifers, crinoids, and gastropods. Ooids with a few fine-radial laminae and intraclasts are also common.

MF6 corresponds to SMF11 of Flügel (2010). Grainstones with a rich and varied fossil assemblage and a high percentage of cortoids, other coated grains, and rounded bioclasts indicate a high-energy depositional environment with persistent wave action (Scholle et al., 1983; Flügel, 2004). Radial ooids suggest a brackish, low-energy lagoonal environment instead. Intraclasts are most common in the intertidal zone, where they may represent the product of tidal-flat erosion and redeposition by storms. (Figure 4G). These mixed features indicate shallow-marine, high-energy beach environments facing the open sea and deposition above fair-weather waves (depth indicatively not >15–20 m; Tucker and Wright, 2009).

4.2.6 MF7 (sandy) wackestone/floatstone

MF7 consists of grayish-green marlstone in the lower part of the Kalataer Formation. Detrital quartz with fragments of mudrock and chert (0%–15%) occur with common bioclasts (10%–35%), including bivalves, crinoids, and a few bryozoans, coralline algae, and small benthic foraminifers. Clasts mainly range between 0.2 and 1.5 mm but are locally >2 mm. The matrix is mixed micrite and terrigenous clay. Bioturbation is common (Figures 4C, D). The fossil assemblage and common bioturbation point to a relatively enclosed inner neritic subtidal environment adjacent to a lagoon.

4.2.7 MF8 bioclastic rudstone

MF8 consists of grayish-green, thick-bedded bioclastic limestone commonly intercalated with MF1 in the middle or upper parts of the upper member of the Kalataer Formation. Carbonate grains (45%–55%) are dominated by oysters (*Turkostres*) commonly larger than 2 mm, associated with planktonic foraminifers, filaments, serpulids, crinoids, bryozoans, ostracods, and small benthic foraminifers. Matrix is micrite with minor terrigenous silt (Figure 4H).

MF8 corresponds to SMF12–S of Flügel (2010). Although oysters, which are widespread throughout the western Tarim Basin (Zhang et al., 2018), generally thrive in warm shallow seas (Lan and Wei, 1995), the abundance of background micrite, planktonic foraminifers, and

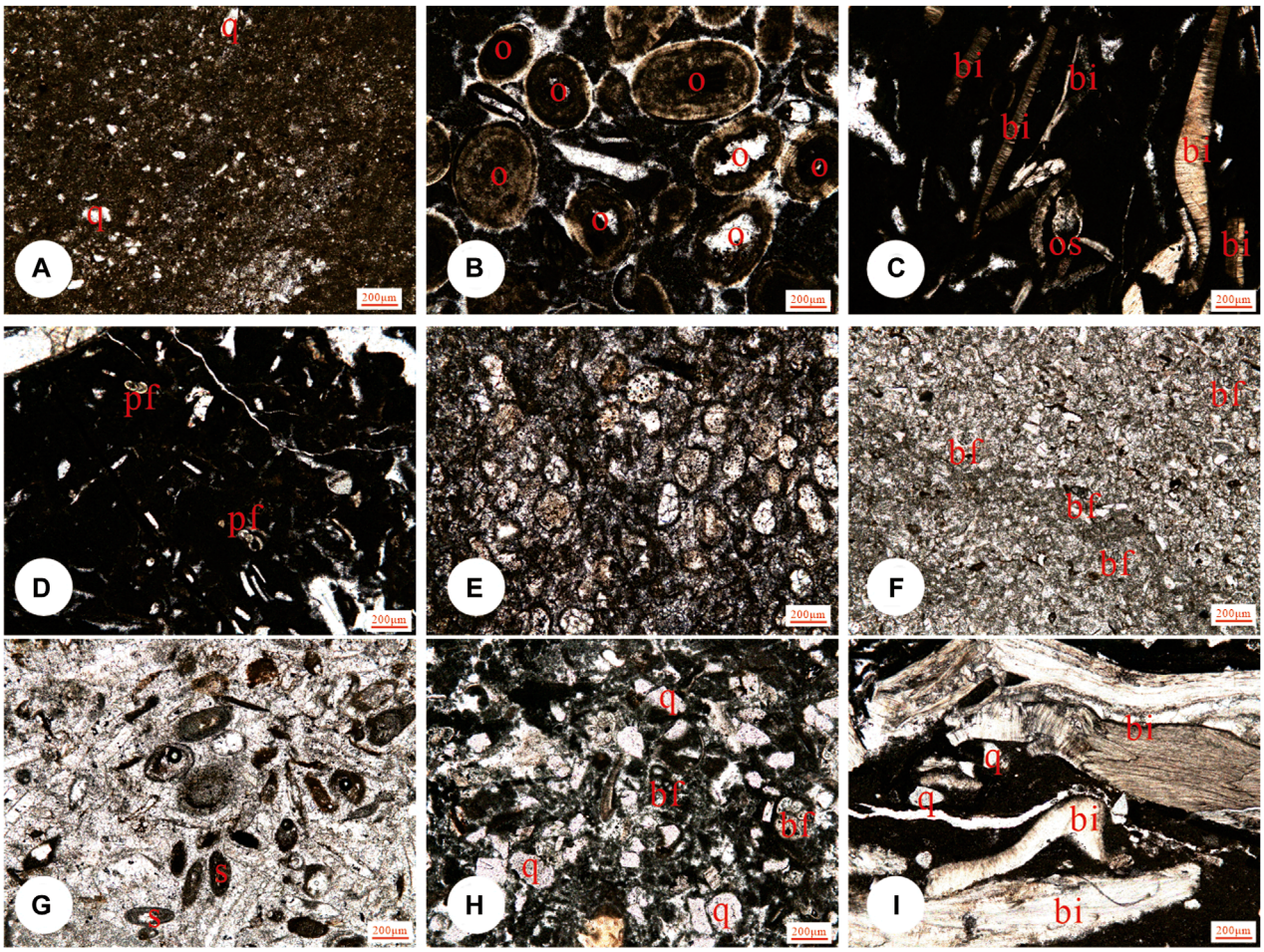

FIGURE 4
Representative microfacies in the Kalataer Formation: **(A)** MF3 mudstone, **(B)** MF4 Oolite grainstones, **(C, D)** MF7 (Sandy) wackestone/floatstone, **(E)** MF2 dolostone (tidal flat, sabkha), **(F)** MF5 bioclastic grainstone, **(G)** MF6 bioclastic grainstone, **(H)** MF8 bioclastic wackestone, and **(I)** MF9 bivalve floatstone/rudstone. Scale bar:200 μm. Key: pf, planktic foraminifera; bf, benthic foraminifera; q, quartz; br, bryozoan; bi, bivalve; s, serpulid; e, echinoderm; a, algae.

filaments point to a deeper-water depositional environment (Van der Zwaan et al., 1990).

4.3 Open marine platform

4.3.1 MF9 bivalve floatstone/rudstone (oyster bed) (slope)

MF9 is a grayish-white oyster bed with a micrite matrix (Figure 4I), ranging in thickness from decimeters to 12 m. Thicker layers are generally intact, whereas thin layers are commonly broken. *Ostrea* (*Turkostrea*) is widespread throughout the western Tarim Basin. Specimens are commonly 2–6 cm in size (but range from 1 cm to >10 cm), well-preserved, stacked onto each other, and heavily burrowed.

MF9 corresponds to SMF12–Bs of Flügel (2010). Banks of *Ostrea* (*Turkostrea*) grew on hard ground in warm, shallow seas (Lan and Wei, 1995). Dendritic bryozoans, intact serpulid worm tubes, and uniform micrite matrix all indicate weak hydrodynamic conditions (Scholle and Ulmer-Scholle, 2003).

5 Biostratigraphy and paleoecology

5.1 Biostratigraphy

5.1.1 Bivalves

Three genera and seven species (two subspecies) were identified from the Kalataer Formation (Figure 5), including *Ostrea* (*Turkostrea*) *baissuensis* Vyalov, *Ostrea* (*Turkostrea*) *cizancourti* Cox, *Ostrea* (*Turkostrea*) *strictiplicata* Roulin et Delbos, *Ostrea* (*Turkostrea*) *strictiplicata alaica* Vyalov, *Ostrea* (*Turkostrea*) *strictiplicata borgalensis* Vyalov, *Kokanostrea kokanensis* (Sokolov), and *Sokolowia buhsii* (Grewingk). Three assemblages of bivalves were identified in the Kalataer Formation: *Ostrea* (*Turkostrea*) *strictiplicata*, *Ostrea* (*Turkostrea*) *cizancourti*–*Ostrea* (*Turkostrea*) *strictiplicata*, and an *Ostrea* (*Turkostrea*) *strictiplicata*–*S. buhsii* assemblage.

An *Ostrea* (*Turkostrea*) *strictiplicata* assemblage appears in the middle part of the Kalataer Formation, characterized by the appearance of abundant *Ostrea* (*Turkostrea*) *strictiplicata*

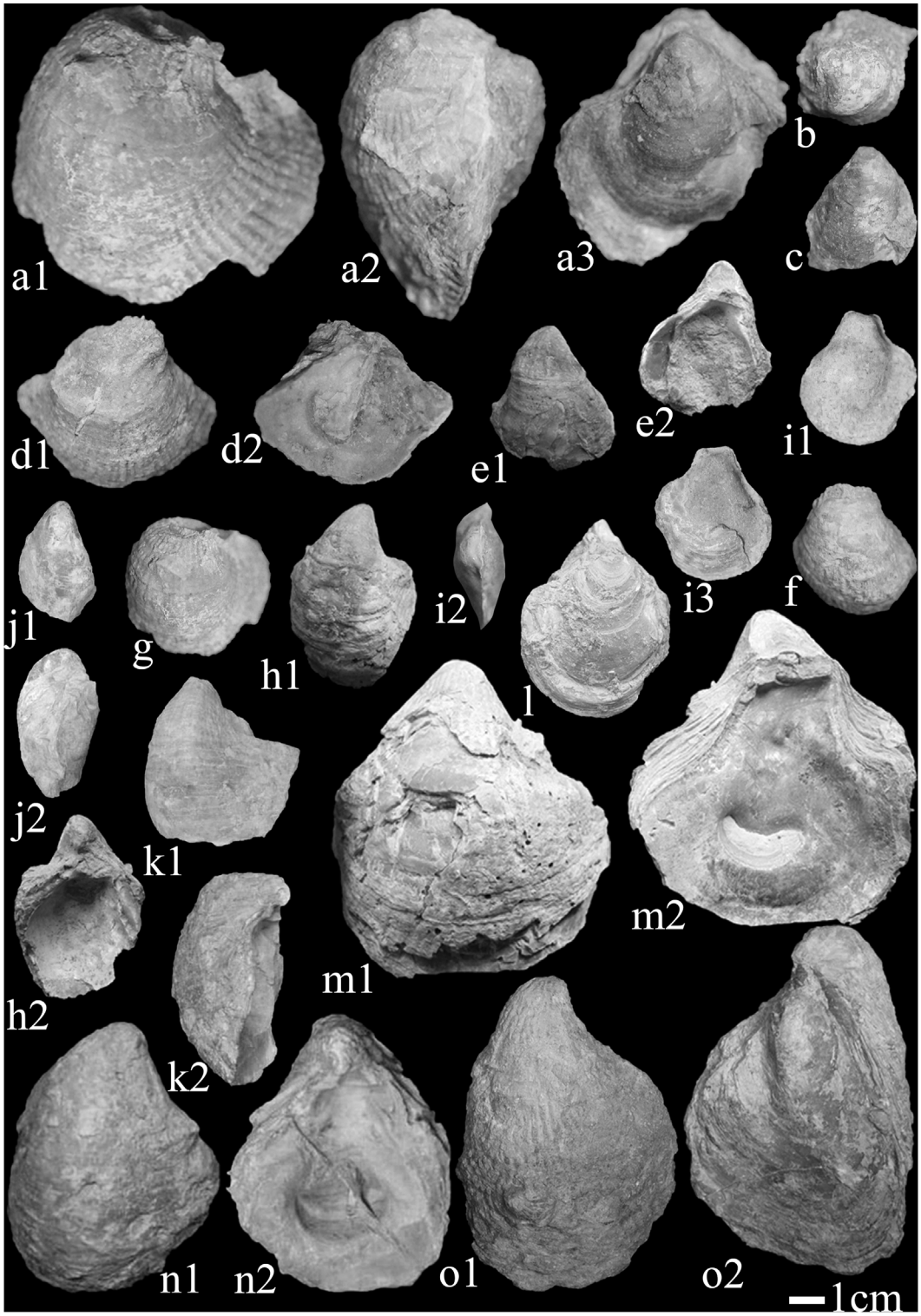

FIGURE 5
Representative bivalves in the Kalataer Formation (1 cm scale). a-c,e-g i, *Ostrea (Turkostrea) baissuensis* Vyalov; d, *Ostrea (Turkostrea) cizancourti* Cox; h, *Ostrea (Turkostrea) strictiplicata alaica* Vyalov; j. *Kokanostrea kokanensis* (Sokolov); k. *Ostrea (Turkostrea) strictiplicata* Roulin et Delbos; l, m, *Sokolowia buhsii* (Grewingk); n, *Ostrea (Turkostrea) strictiplicata* Roulin et Delbos; o, *Ostrea (Turkostrea) strictiplicata borgalensis* Vyalov.

(approximately 2–4 cm in length or high) individuals. An *Ostrea* (*Turkostrea*) *cizancourti*–*Ostrea* (*Turkostrea*) *strictiplicata* assemblage appears in the low upper part of the Kalataer Formation, marked by the appearance of *Ostrea* (*Turkostrea*) *strictiplicata*. An *Ostrea* (*Turkostrea*) *strictiplicata*–*S. buhsii* assemblage appears in the middle-upper part of the Kalataer Formation, marked by the

appearance of *S. buhsii*. These assemblages are consistent with the *Turkostrea–Ostrea* or *Ostrea* (*Turkostrea*) *turkestanensis* assemblage established by Wei (1982) and Wu (1991).

Among them, *Sokolowia* shows a rapid evolution, with a short duration being restricted to the middle-late Eocene of Central Asia and Romania (Berizzi Quarto di Palo, 1970; Stenzel, 1971; Lan, 1997; Rusu et al., 2004; Bosboom et al., 2011; Salahi and Vahidinia, 2011). *Ostrea* (*Turkostrea*) *strictiplicata* Roulin et Delbos was once found in the Alai layer in Central Asia, and its age is in the middle Eocene (Tang et al., 1989). *Ostrea* (*Turkostrea*) *strictiplicata* Raulin et Delbosa, in addition to being distributed in the Fergan, Tajik Basin, Tashkent, and Aleyi Mountains in Central Asia, is also distributed in Afghanistan, southern Iran, and North Africa from the middle and lower Eocene (Wei, 1982; Lan and Wei, 1995; Lan, 1997).

5.1.2 Foraminifers

In our work, we identified three genera and five species of small benthic foraminifers in the middle part of the Kalatar Formation, and eight genera and 15 species of the small benthic foraminifers made into two assemblages in the upper part of the Kalatar Formation (Figure 6).

5.1.2.1 *Quinqueloculina–Miliola–Oolina assemblage*

In the middle part of the Kalatar Formation, *Quinqueloculina* and other taxa, such as *Miliola* and *Oolina* species, display moderate to poorly preserved tests. These taxa are not abundant. In this section, we only identified *Quinqueloculina striata*, *Quinqueloculina* spp., *Miliola birostris*, *Oolina stellula*, and *Oolina* sp.

5.1.2.2 *Elphidium–Cibicides–Nonion assemblage*

A large number of porcelainous small benthic foraminifers appeared at the top part of the Kalatar Formation. These forms are common in neritic. In this assemblage, we identified abundant *Elphidium laeve*, *Cibicides artemi*, and *Nonion laevigatum*. *Elphidium cynicalis*, *Elphidium hiltermanni*, *Nonion formosum*, and *Cibicides entendus* also appear.

5.1.2.3 *Anomalina–Melonis–Pullenia assemblage*

Pullenia is the dominant genera in this assemblage. We identified *Pullenia bulliodes* and *Melonis larvigatus*, *Melonis* spp., *Anomalina samanica*, *Anomalina subaequalis*, *Anomalina trunicata*, and *Anomalinoides pertalifermis* appeared at the same time.

5.1.3 Gastropods

The gastropod fauna is relatively poor and exclusively occurs in the upper part of the Kalatar Formation. The assemblage is mainly dominated by the genera *Cerithium* and *Niso* (Tang et al., 1989). The establishment of the *Cerithium tristichum–Niso constricta* assemblage (Tang et al., 1989) was mainly marked by the appearance of *C. tristichum* and *Ficus* cf. *crassistria* (Koenen). *Cerithium tristichum Bagmanov* was originally produced in the lower Eocene of the Lesser Caucasus, and *Ficus* cf. *crassistria* (Koenen) is also found in the Paleocene of the Middle Carpathians. *Niso constricta* (Desahaye) was first discovered in the lower Eocene (Cuisian) of the Paris Basin and the middle and lower Eocene of Ukraine. It is more appropriate to attribute it to the early Eocene (Tang et al., 1989).

During the middle Eocene, the Tarim Basin was covered by oyster biostromes. *Ostrea* (*Turkostrea*) spp. are dominant in the limestone and were also found in the Middle Eocene Alai Bed of Central Asia and northern Afghanistan. They are associated with the gastropod *C. tristichum–N. constricta* assemblage of the Lower Eocene and *N. constricta* described from the Cuisian of the Paris Basin. They also occur in the Middle and Lower Eocene of Ukraine with the foraminifers *Anomalinoides*, *C. entendus*, and *C. artemi*, which are common elements in the Eocene of Paris Basin. Therefore, the assemblage belongs to the early middle Eocene. Above all, based on multi-phyla fossil records, the Kalatar Formation is Lutetian in age.

5.2 Paleoecology

The gypsum and evaporites are mainly interbedded in the lower part of the Kalatar Formation. Fauna cannot survive in such strict conditions. This usually indicates a semi-arid climate and saline environment (Zhang et al., 2018). In the upper lower part of the Kalatar Formation, only *Cerithium*, *Ficus,* and *Niso* have been found in the Bashibulake districts (Figures 7A–J). Living representatives of these genera are found on sand and muddy substrates of tropical and subtropical tidal flats (Houbrick, 1974). Therefore, this assemblage is thought to have lived in a similar environment or possibly on the inner gulf with a water depth of up to 10 m. Gastropods are indicative of a soft-muddy and sandy substrate that is interpreted as either back shoal or subtidal shallow warm water (Pan et al., 1991).

In the middle part of the Kalatar Formation, *Ostrea* (*Turkostrea*) *strictiplicata* are relatively small. The genus and species are monotonous due to elevated salinity and muddy elements and indicate deposition of the middle part of the Kalatar Formation at a very shallow depth. In the *Quinqueloculina–Miliola–Oolina* assemblage, all these taxa have been reported as shallow water taxa for recent sediment (Murray, 1991; 2006; Thomas, 1998). The porcelaneous and agglutinated species did not appear at that time. Only hyaline species appear, indicating the environment was strict in this period, with higher salinity, which was not suitable for the survival of porcelaneous and agglutinated species. Only hyaline species can be preserved (Van der Zwaan et al., 1990; Gooday, 2003; Jorissen et al., 1995; 2007; Widmark and Speijer, 1997; Thomas et al., 1998). *Quinqueloculina* and *Miliola* are hyaline genera. The walls are formed by the crystallization of carbonate minerals secreted by themselves, but the mineral crystals are arranged disorderly on the walls, and the crystal columns are randomly distributed. This disorder makes the formed walls relatively strong and sturdy, resembling porcelain in appearance, and gives them the ability to resist harsh external conditions (Berggren and Aubert, 1975; Tjalsma and Lohmann, 1983; Van Morkhoven et al., 1986). Therefore, when other species disappear one after another, *Quinqueloculina* and *Miliola* can thrive in large numbers, which is not only related to the protective effect of their shell walls; they may also have more physiological and biochemical mechanisms to tolerate harsh environments. *Quinqueloculina* and *Miliola* most likely lived in up to 50-m-deep neritic and hypersaline conditions. Some lived in normal marine lagoons and carbonate platforms, whilst *Oolina* can live in a wider range (Tjalsma and Lohmann, 1983; Van Morkhoven et al., 1986; Murray, 2006). Abundant porcelaneous foraminifer tests,

10.3389/feart.2024.1398474

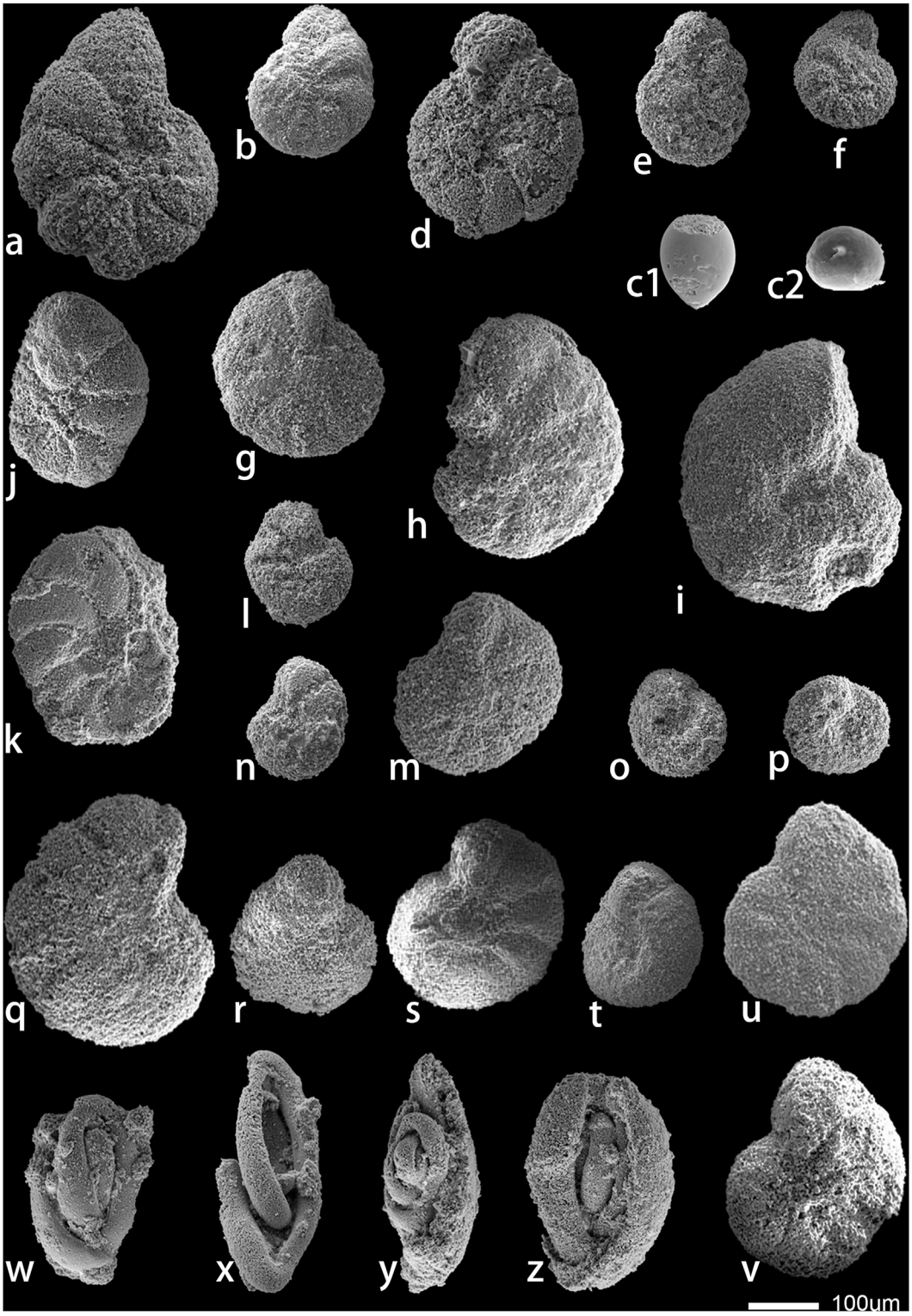

FIGURE 6
Representative foraminifers in the Kalataer Formation. a-b, d, *Elphidium hiltermanni*; c1, *Oolina stellula*; c2, *Oolina* sp.; e, *Elphidium laeve*; f, *Elphidium cynicalis*; g-h, *Nonion formosum*; i, *Nonion* sp.; j, *Nonion laevigatum*; k, *Cibicides artemi*; l, *Cibicides entendus*; m-n, *Anomalina samanica*; o-p, *Pullenia bulliodes*; q, *Anomalina subaequalis*; r, *Anomalina trunicata*; s, *Anomalinoides pertalifermis*; t-u, *Melonis* spp.; v, *Melonis larvigatus*; w, *Quinqueloculina* spp., x, *Miliola birostris*; y, *Quinqueloculina* spp.; z, *Quinqueloculina striata*.

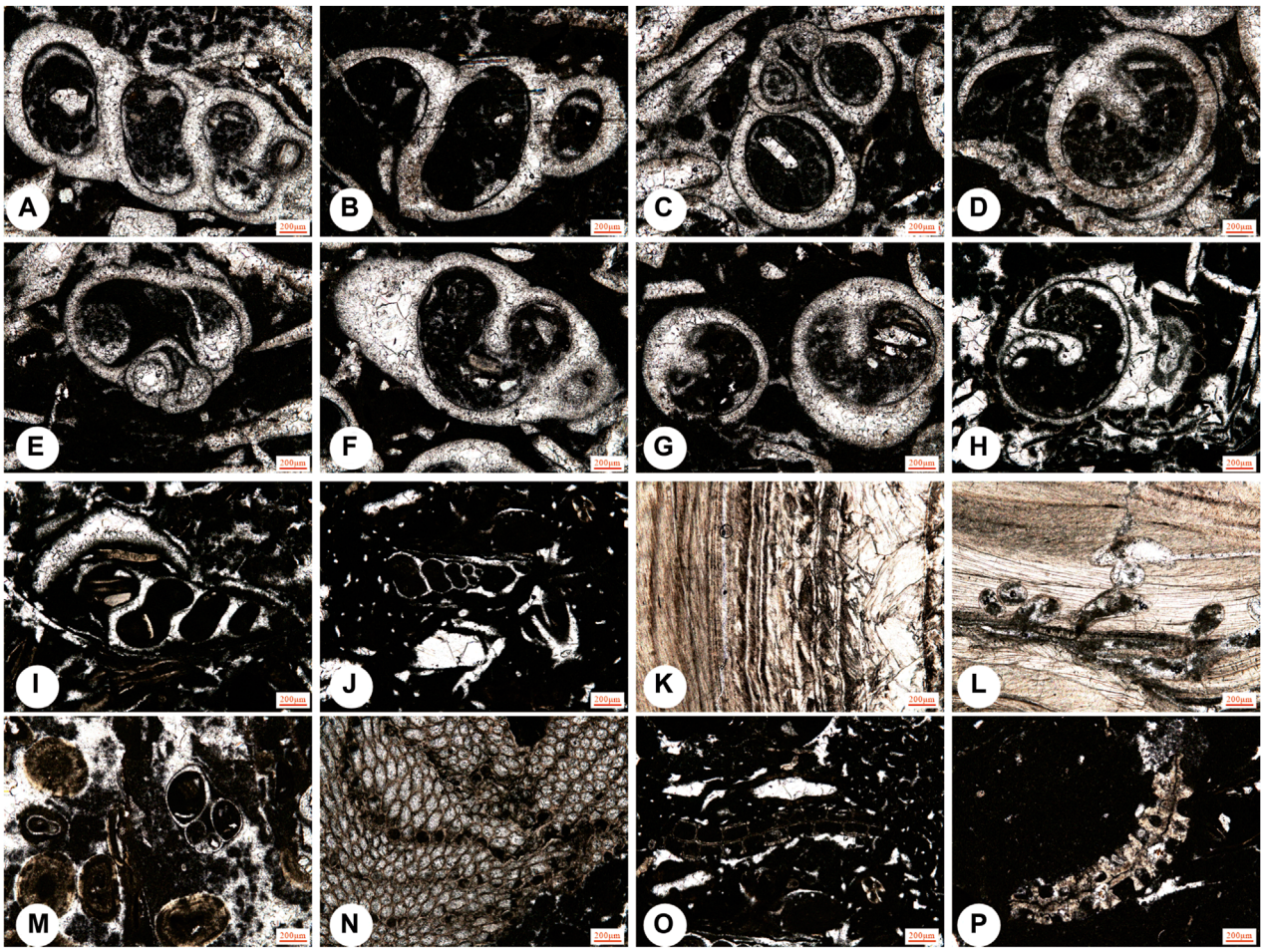

FIGURE 7
Representative fossils in the Kalataer Formation. **(A–J)** j, *Niso contricta Deshayes*; m, gastropods; **(K–L)** Micro-borings in oyster fragments; **(N–P)** bryozoan.

especially *miliolids*, indicate low turbulence, warm water in restricted settings, and, in turn, slightly hypersaline conditions (Jorissen et al., 1995). It can be associated with a hypersaline lagoon environment.

In the low upper part of the Kalataer Formation, *Ostrea* (*Turkostrea*) *cizancourti* varies in size, and the genus and species are monotonous. The *Ostrea* (*Turkostrea*) *cizancourti–Ostrea* (*Turkostrea*) *strictiplicata* assemblage living in the low part of the intertidal and hard ground shows that the environment could be clear and warm sea water in the lower upper part of the Kalataer Formation. In the *Elphidium–Cibicides–Nonion* assemblage, species of *Elphidium* mostly like living in shallow sea environments ranging from 0 m to 10 m, with some living in shelf seas ranging from 0 m to 50 m (Tjalsma and Lohmann, 1983; Arreguín-Rodríguez and Alegret, 2016). Recent *Cibicides* species have an epifaunal mode of life and are usually attached to and inhabiting elevated microhabitats, fixed to animals, plants, or hard substrates like pebbles (Murray, 1991; 2006; Schweizer, 2006). The species of *Cibicides* are most abundant in waters of the phototropic zone, down to approximately 50 m in clear waters of temperate regions, with *Nonion* living in a wide range (Hao et al., 1982; Jorissen et al., 1995; Tosquella et al., 2022). This indicates that their locale belongs to a normal shallow-shelf sea.

In the upper part of the Kalataer Formation, *Sokolowia* was an epibenthic and suspension feeder characterized by massive and large-sized shells. It was well adapted to solitary life in the subtidal shallow marine water conditions, with their left valves lying on soft-muddy and sandy bottoms, partially sunk into the substratum, whereas their flat right valves attained a nearly horizontal position (Stenzel, 1971; Lan, 1997; Rusu et al., 2004; Bosboom et al., 2011). Several authors also pointed out that *Sokolowia* lived in normal salinity conditions in a deeper part of the shallow water zone under the influence of wave action (e.g., Stenzel, 1971; Mészáros et al., 1987; Lan, 1997). Their thick-walled, heavy shells made them practically immovable by water turbulence at the sea bottom (Hadi et al., 2019). The individuals vary in size, and the genus and species are monotonous. Due to reduced salinity, increased muddy elements, and turbulent water, *Turkostrea* was reduced in number whilst *Sokolowia* became abundant. In the *Anomalina–Melonis–Pullenia* assemblage, *Cibicides* concentrated in warm waters at depths of 20–50 m, while the rest were *Anomalina* and *Melonis*. *Pullenia* live in deeper areas of seawater

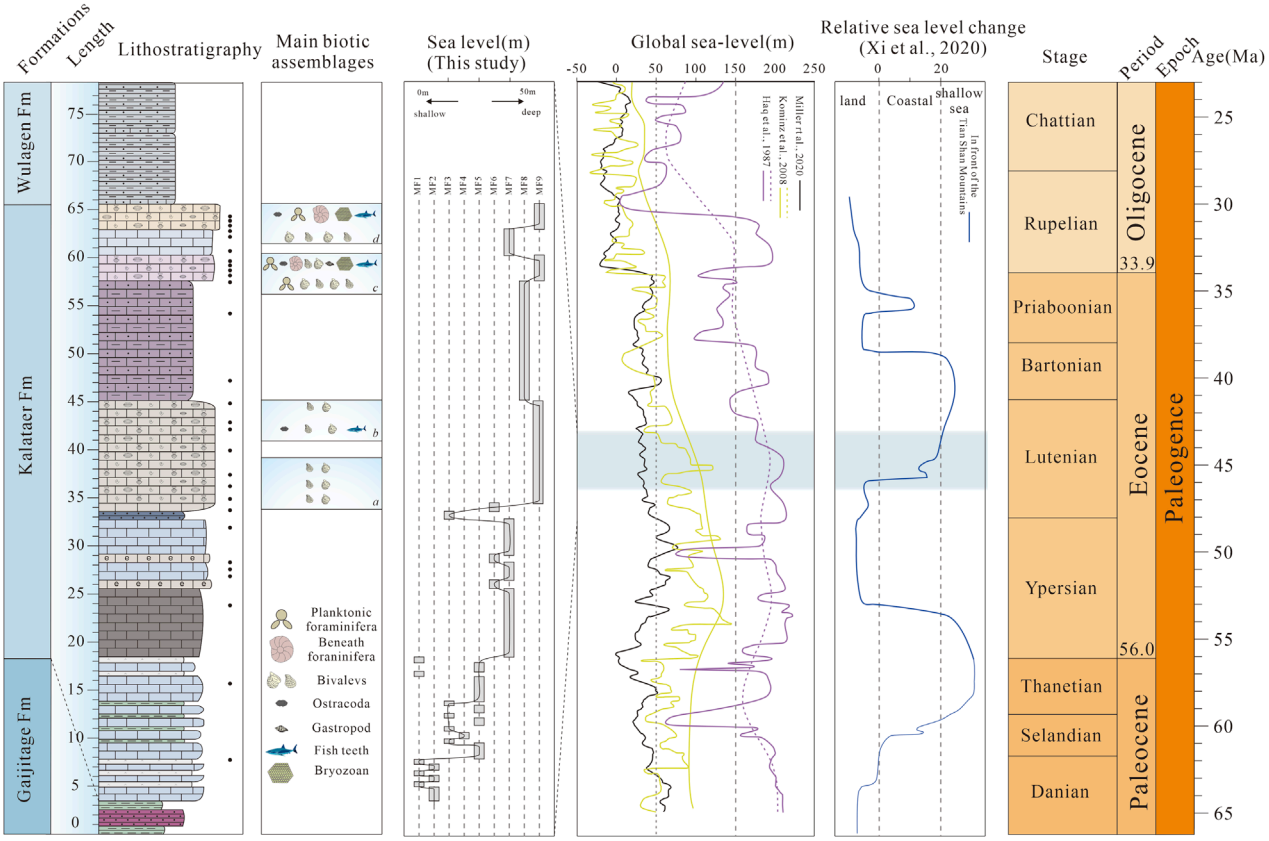

FIGURE 8
Representative transgression in the Kalataer Formation and comparison of relative sea-level or paleodepth curves for the Paleogene. The global sea level change is from Haq et al. (1987), Kominz et al. (2008),and Miller et al. (2020). The sea level change in front of the Tian Shan Mountains is from Xi et al. (2020).

(Hao et al., 1982; Thomas, 1998; Boscolo Galazzo et al., 2013; 2015). The abundance of *Pullenia* and *Melonis* in the upper part of the Kalataer Formation indicates that rather deeper-water conditions prevailed at the peak of the Kalataer transgression.

In the mid-Eocene, the western part of the Tarim Basin was a narrow bay, although connected with the Tethys Sea. Its geographical isolation led to the presence of some local species in this area (Berggren and Aubert, 1975; Hao et al., 1982; Tjalsma and Lohmann, 1983; Murray, 1991; Lan and Wei, 1995; Xi et al., 2020). At that time, this area was again transgressed from the east Mediterranean subprovince. In the beginning, this area was under semi-arid climates and a saline environment in which fauna could not survive. As the transgression continued, more varied benthonic faunas became dominant. The biota of the Kalataer Formation mainly lived in open shallow sea environments, with medium to low energy and rich nutrients and oxygen, representing a typical shallow marine ecosystem of a carbonate platform (Figure 9A).

6 Discussion

Previous studies have demonstrated that during the Paleogene, a seaway existed between the Tarim Sea, the Western Tethys, and the Arctic Ocean (e.g., Bosboom et al., 2011; Bosboom et al., 2014a; 2014b; 2014c; 2017; Carrapa et al., 2015; Kaya et al., 2019; Zhang et al., 2022). At the same time, the marine fossil assemblages from the western Tarim Basin show strong similarities with contemporaneous Eurasian basins (Bosboom et al., 2011; Bosboom et al., 2014a) (Figure 9B, C). Deposits widely distributed in the western Tarim Basin are shallow sea nearshore facies, including terrigenous sediments, evaporites, and carbonates, with bivalves, gastropods, brachiopods, bryozoans, serpulids, echonoids, crinoids, ostracods, foraminifers, dinoflagellates, calcareous algae, calcareous nannoplanktons, sporepollens, fish teeth, and crustaceans (Hao et al., 1982; 2001; Mao and Norris, 1988; Tang et al., 1989; 1992; Guo, 1990; 1995; Zhong, 1992; Jiang et al., 1995; Lan and Wei, 1995; Yang et al., 1995; Bosboom et al., 2011; Yang et al., 2012; Sun and Jiang, 2013; Wang et al., 2014). Bivalve and foraminiferal fossils exhibit sensitivity to environmental changes, thereby serving as reliable indicators of the paleoenvironmental conditions within the Kalataer Formation.

In our work, microfacies analysis indicates that the Kalataer Formation experienced a transgressive event in the Bashibulake Section (Figure 8). Gypsum layers deposited in sabkha environments (MF1, MF2) are overlain by supratidal dolomitic mudstones (MF3) at the lower part of the Kalataer Formation. Above, oolite grainstones (MF4) were deposited in a relatively stable environment, perhaps adjacent to an oolitic shoal,

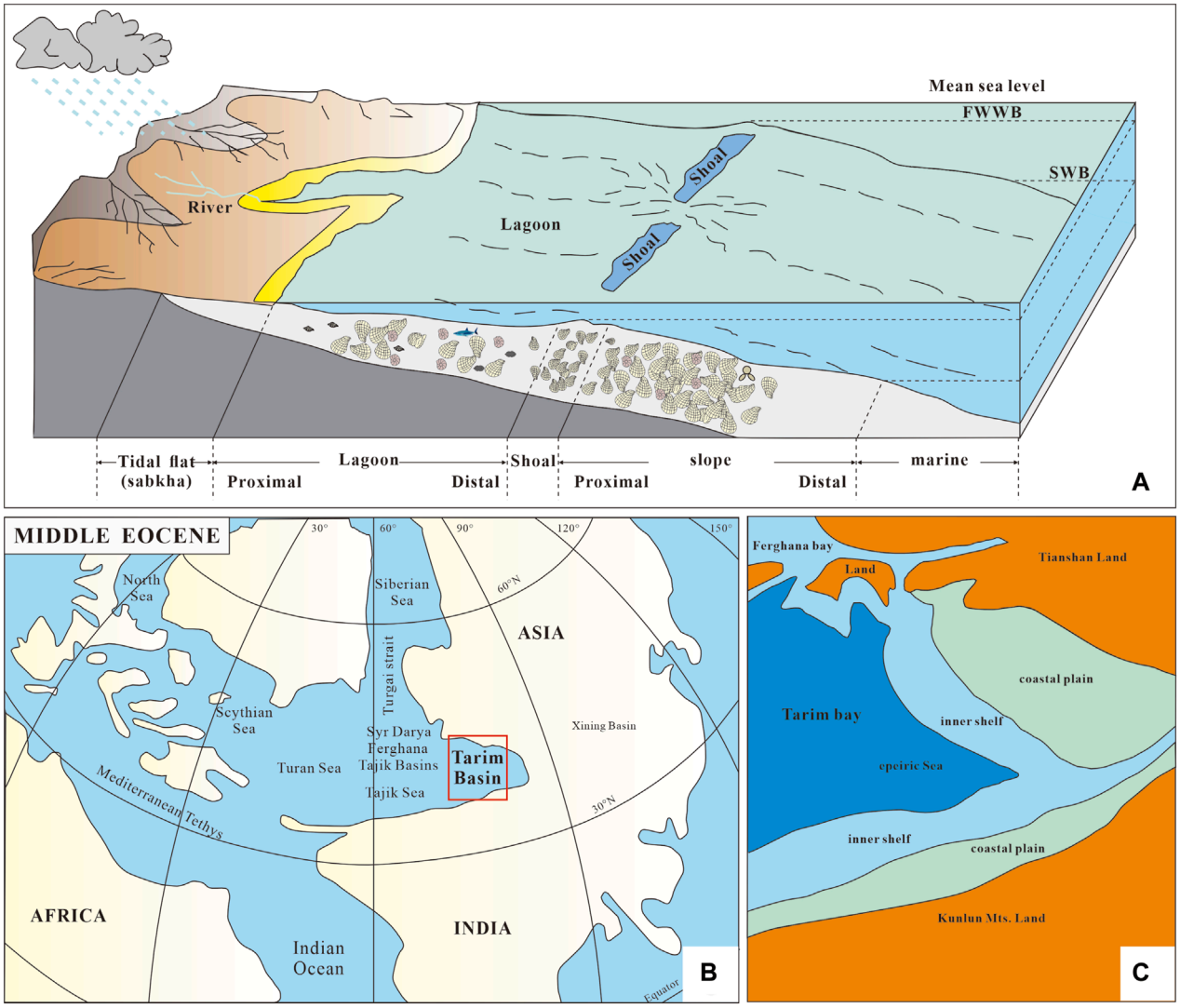

FIGURE 9
(A) Sedimentary environment pattern of the Kalataer Formation; **(B, C)** preliminary paleogeographic maps of the Tarim Basin and adjacent areas in the middle Eocene (after Sobel, 1999; Tang et al., 1989; Bosboom et al., 2017; Xi et al., 2016; 2019; Jiang et al., 2018).

whereas wackestone and mudstone with fine exposed laminations accumulated in subtidal to lagoonal environments (MF5, MF6, MF7). After this period of relatively limited depositional conditions in the Bashibulake Section, bioclastic wackestone/floatstone and bioclastic rudstone with abundant shallow marine fossils (MF7, MF8) indicate a transition to an open-marine inner ramp, followed by bivalve floatstone/rudstone (oyster bed) deposited on a slope (MF9) (Figure 9A). Sedimentary microfacies analysis is consistent with paleontological evidence, and the transgression process is consistent with that described by Xi et al. (2020), but it is not consistent with global sea level change (Figure 8).

The Paleogene sea distribution progressively decreases, corresponding to the global trends of sea level fluctuation. Two main controlling mechanisms have previously been proposed for the relative sea level change of the Tarim Sea: a tectonic link to the India–Asia collision and a eustatic sea-level link to global climate (e.g., Bosboom et al., 2014b; Zhang et al., 2018; 2019; Kaya et al., 2019). According to recent studies (Cretaceous to Paleongene), the fourth major late Eocene (early Bartonian) sea retreat was controlled by a combination of normal regression driven by excess sediment supply related to tectonism and a forced regression related to a net eustatic sea-level fall (e.g., Haq et al., 1987; Kominz et al., 2008; Miller et al., 2020), but the mechanism of temporary transgression in the middle Eocene is still unknown. We considered that this transgression may be caused simultaneously by global sea level rise and regional tectonic movements.

7 Conclusion

Bivalves and the small benthic foraminifer assemblages of *Ostrea* (*Turkostrea*) *strictiplicata, Ostrea* (*Turkostrea*) *cizancourti–Ostrea* (*Turkostrea*) *strictiplicata,* and *Ostrea* (*Turkostrea*) *strictiplicata–S. buhsii*, the small benthic foraminifer assemblages of

Quinqueloculina–Miliola–Oolina, the *Elphidium–Cibicides–Nonion* assemblage, and the *Anomalina–Melonis–Pullenia* assemblage indicate the age of the Kalataer Formation is middle Lutetian of the Eocene.

By integrating fossil assemblages with corresponding sedimentary lithologies, we have delineated nine distinct sedimentary microfacies (MF1 to MF9). These microfacies epitomize a gradient of environmental conditions, ranging from semi-confined to expansively open shallow marine settings characterized by medium to low energy dynamics. The biotic communities inhabiting the Kalataer Formation are predominantly found in these open, shallow marine environments, which are distinguished by their medium to low energetic ambiance and are abundantly endowed with nutrients and oxygen. This configuration typifies a quintessential ecosystem associated with a carbonate platform.

The microfacies and fossil assemblages suggest a shallow marine epicontinental paleoenvironment with connections to the adjacent Tethyan Sea during the middle Eocene in the western Tarim Basin (Figure 9B, C), and a large marine transgression event occurred. This transgression may be caused simultaneously by global sea level rise and regional tectonic movements.

Data availability statement

The datasets presented in this study can be found in online repositories. The names of the repository/repositories and accession number(s) can be found in the article/supplementary material.

Ethics statement

The manuscript presents research on animals that do not require ethical approval for their study.

Author contributions

SF: data curation, formal analysis, investigation, software, validation, writing–original draft, and writing–review and editing. DX: investigation, project administration, writing–original draft, writing–review and editing, funding acquisition, and supervision. QS: writing–original draft. DLL: writing–review and editing. ZY: writing–review and editing. DNL: writing–review and editing and investigation. YW: writing–review and editing and investigation. TJ: writing–review and editing, funding acquisition, and project administration. XW: writing–review and editing.

Funding

The author(s) declare that financial support was received for the research, authorship, and/or publication of this article. This study was supported by the National Natural Science Foundation of China (42072001, 42272035), the Chinese "111" project, and the International Geological Comparison Program (IGCP679).

Acknowledgments

The authors would like to thank the two reviewers for their constructive comments and helpful suggestions that greatly improved the manuscript. They also thank Xiao Ziyuan and Ning Yafeng for their help in the laboratory work.

Conflict of interest

Authors DLL and ZY were employed by Shaanxi Geology and Mining First Geological Team Co., Ltd.

The remaining authors declare that the research was conducted in the absence of any commercial or financial relationships that could be construed as a potential conflict of interest.

Publisher's note

References

Arreguín-Rodríguez, G. J., and Alegret, L. (2016). Deep-sea benthic foraminiferal turnover across early Eocene hyperthermal events at northeast Atlantic DSDP site 550. *Palaeogeogr. Palaeoclimatol. Palaeoecol.* 451, 62–72. doi:10.1016/j.palaeo.2016.03.010

Berggren, W. A., and Aubert, J. (1975). Paleocene benthonic foraminiferal biostratigraphy, paleobiogeography and paleoecology of Atlantic–Tethyan regions: midway–type fauna. *Palaeogeogr. Palaeoclimatol. Palaeoecol.* 18, 73–192. doi:10.1016/0031-0182(75)90025-5

Berizzi Quarto di Palo, A. (1970). "Paleogene pelecypods from kataghan and badakhshan (North-East afganistan)," in *Fossils of north-east afganistan: Italian expeditions to the karakorum (K2), and hindu kush, IV/2* (Leiden: Brill), 161–240.

Bosboom, R., Dupont-Nivet, G., Grothe, A., Brinkhuis, H., Villa, G., Mandic, O., et al. (2014a). Timing, cause and impact of the late Eocene stepwise sea retreat from the Tarim Basin (west China). *Palaeogeogr. Palaeoclimatol. Palaeoecol.* 403, 101–118. doi:10.1016/j.palaeo.2014.03.035

Bosboom, R. E., Abels, H. A., Hoorn, C., van den Berg, B. C. J., Guo, Z. J., and Dupont–Nivet, G. (2014b). Aridification in continental Asia after the middle Eocene climatic optimum (MECO). *Earth Planet. Sci. Lett.* 389, 34–42. doi:10.1016/j.epsl.2013.12.014

Bosboom, R. E., Dupont–Nivet, G., Grothe, A., Brinkhuis, H., Villa, G., Mandic, O., et al. (2014c). Linking Tarim Basin sea retreat (west China) and Asian aridification in the late Eocene. *Basin Res.* 26, 621–640. doi:10.1111/bre.12054

Bosboom, R. E., Dupont–Nivet, G., Houben, A. J. P., Brinkhuis, H., Villa, G., Mandic, O., et al. (2011). Late Eocene sea retreat from the Tarim Basin (west China) and concomitant asian paleoenvironmental change. *Palaeogeogr. Palaeoclimatol. Palaeoecol.* 299, 385–398. doi:10.1016/j.palaeo.2010.11.019

Bosboom, R. E., Mandic, O., Dupont–Nivet, G., Proust, J. N., Ormukov, C. A., and Aminov, J. (2017). *Late Eocene paleogeography of the proto–paratethys sea in central Asia (NW China, S Kyrgyzstan and SW Tajikistan)*. Burlington House, Piccadilly London: Geological Society Special Publication, 565–588. doi:10.1144/SP427.11

Boscolo Galazzo, F., Giusberti, L., Luciani, V., and Thomas, E. (2013). Paleoenvironmental changes during the Middle Eocene Climatic Optimum (MECO) and its aftermath: the benthic foraminiferal record from the Alano section (NE Italy). *Palaeogeogr. Palaeoclimatol. Palaeoecol.* 378, 22–35. doi:10.1016/j.palaeo.2013.03.018

Boscolo Galazzo, F., Thomas, E., and Giusberti, L. (2015). Benthic foraminiferal response to the middle Eocene climatic optimum (MECO) in the south–eastern atlantic (ODP site 1263). *Palaeogeogr. Palaeoclimatol. Palaeoecol.* 417, 432–444. doi:10.1016/j.palaeo.2014.10.004

Cao, W. X., Xi, D. P., Melinte–Dobrinescu, M. C., Jiang, T., Wise, S. W., and Wan, X. Q. (2018). Calcareous nannofossil changes linked to climate deterioration during the Paleocene–Eocene thermal maximum in Tarim Basin, NW China. *Geosci. Front.* 9, 1465–1478. doi:10.1016/j.gsf.2018.04.002

Carrapa, B., DeCelles, P. G., Wang, X., Clementz, M. T., Mancin, N., Stoica, M., et al. (2015). Tectono–climatic implications of Eocene Paratethys regression in the Tajik basin of central Asia. *Earth Planet. Sci. Lett.* 424, 168–178. doi:10.1016/j.epsl.2015.05.034

Davies, R. B., Casey, D. M., Horbury, A. D., Sharland, P. R., and Simmons, M. D. (2002). Early to mid–Cretaceous mixed carbonate–clastic shelfal systems: examples, issues and models from the Arabian Plate. *GeoArabia* 7, 541–598. doi:10.2113/geoarabia0703541

Dunham, R. J. (1962). Classification of carbonate rocks according to deposition texture. *Mem. Am. Assoc. Petroleum Geol.* 1, 108–121.

Embry, A. F., and Klovan, J. E. (1971). A late devonian reef tract on northeastern banks island, N. W. T. *Bull. Can. petroleum Geol.* 19, 730–781. doi:10.35767/gscpgbull.19.4.730

Flügel, E. (2004). *Microfacies of carbonate rocks: analysis, interpretation and application*. Berlin, Germany: Springer Science, Business Media, 1–882.

Flügel, E. (2010). *Microfacies of carbonate rocks: analysis, interpretation and application*. Berlin, Germany: Springer Science, Business Media, 1–976.

Ghabeishavi, A., Vaziri-Moghaddam, H., Taheri, A., and Taati, F. (2010). Microfacies and depositional environment of the Cenomanian of the Bangestan anticline, SW Iran. *J. Asian Earth Sci.* 37, 275–285. doi:10.1016/j.jseaes.2009.08.014

Gooday, A. J. (2003). Benthic foraminifera (protista) as tools in deep-water palaeoceanography: environmental influences on faunal characteristics. *Adv. Mar. Biol.* 46, 1–90. doi:10.1016/S0065-2881(03)46002-1

Guo, X. P. (1990). Study on marine cretaceous–tertiary boundary in the western Tarim Basin (in Chinese). *Earth Sci. J. China Univ. Geosciences* 15, 325–335.

Guo, X. P. (1991). An approach to the depositional environment of the Cretaceous Kizilsu Group: the lowermost marine horizon of the Cretaceous in the western Tarim Basin (in Chinese). *Acta Geol. Sin.* 65, 188–198.

Guo, X. P. (1995). Cretaceous–paleogene foraminiferal communities from the western Tarim Basin and their environmental significance (in Chinese). *Acta Geosci. Sin.* 1, 77–86.

Hadi, M., Salahi, A., Nasiri, Y., and Mosaddegh, H. (2019). *Sokolowia* horizon of the Ziarat Formation (eastern Alborz, Iran): biostratigraphic and paleogeographic implications. *Acta Palaeontol. Rom.* 15, 15–27. doi:10.35463/j.apr.2019.02.02

Hao, Y. C., Guo, X. P., Ye, L. S., Yao, P. Y., Fu, D. R., Li, H. M., et al. (2001). *The boundary between the marine cretaceous and tertiary in the southwest Tarim basin (in Chinese)*. Beijing: Geological Publishing House, 1–108.

Hao, Y. C., and Zeng, X. L. (1984). On the evolution of the West Tarim Gulf from Mesozoic to Cenozoic in terms of characteristics of foraminiferal fauna (in Chinese). *Acta Micropalaeontogica Sin.* 1, 1–16.

Hao, Y. C., Zeng, X. L., and Li, H. M. (1982). Late cretaceous and tertiary strata and foraminifera in western Tarim Basin (in Chinese). *Earth Sci. J. Wuhn Coll. Geol.* 2, 1–161.

Haq, B. U., Hardenbol, J. A. N., and Vail, P. R. (1987). Chronology of fluctuating sea levels since the Triassic. *Science* 235, 1156–1167. doi:10.1126/science.235.4793.1156

Houbrick, R. S. (1974). Growth studies on the genus *Cerithium* (Gastropoda: prosobranchia) with notes on ecology and microhabitats. *Nautilus* 88, 14–27.

Jia, C. Z., Zhang, S. B., and Wu, S. Z. (2004). *Stratigraphy of the Tarim Basin and adjacent areas (in Chinese)*. Beijing: Science Press, 1–450.

Jiang, J. X., Hu, X. M., Li, J., Garzanti, E., Jiang, S. J., Cui, Y., et al. (2023). Eustatic change across the paleocene–eocene thermal maximum in the epicontinental Tarim seaway. *Glob. Planet. Change* 229, 104241. doi:10.1016/j.gloplacha.2023.104241

Jiang, T., Wan, X. Q., Jonathan, C., Aitchison, J. C., Xi, D. P., and Cao, W. X. (2018). Foraminiferal response to the PETM recorded in the SW Tarim Basin, central Asia. *Palaeogeogr. Palaeoclimatol. Palaeoecol.* 506, 217–225. doi:10.1016/j.palaeo.2018.06.041

Jiang, X. T., Zhou, W. F., and Lin, S. P. (1995). *Stratigraphy and ostracods of xinjiang in China (in Chinese)*. Beijing: Geological Publishing House, 1–577.

Jorissen, F. J., de Stigter, H. C., and Widmark, J. G. V. (1995). A conceptual model explaining benthic foraminiferal microhabitats. *Mar. Micropaleontol.* 26, 3–15. doi:10.1016/0377-8398(95)00047-X

Jorissen, F. J., Fontanier, C., and Thomas, E. (2007). "Paleoceanographical proxies based on deep–sea benthic foraminiferal assemblage characteristics," in *Proxies in late cenozoic paleoceanography (Pt. 2): biological tracers and biomarkers*. Editors C. Hillaire–Marcel, and A. de Vernal (Amsterdam, Netherlands: Elsevier).

Kaya, M. Y., Dupont-Nivet, G., Proust, J. N., Roperch, P., Bougeois, L., Meijer, N., et al. (2019). Paleogene evolution and demise of the proto–Paratethys Sea in Central Asia (Tarim and Tajik basins): role of intensified tectonic activity at ca. 41 Ma. *Basin Res.* 31, 461–486. doi:10.1111/bre.12330

Kominz, M. A., Browning, J. V., Miller, K. G., Sugarman, P. J., Mizintseva, S., and Scotese, C. R. (2008). Late Cretaceous to Miocene Sea–level estimates from the New Jersey and Delaware coastal plain coreholes: an error analysis. *Basin Res.* 20, 211–226. doi:10.1111/j.1365-2117.2008.00354.x

Lan, X. (1997). Paleogene bivalve communities in the western Tarim Basin and their paleoenvironmental implications. *Paleoworld* 7, 137–157.

Lan, X., and Wei, J. M. (1995). *The late cretaceous–early tertiary marine bivalve fauna from the western Tarim Basin, south xinjiang, China (in Chinese)*. Beijing: Science Press, 1–214.

Li, Z., Song, W. J., Peng, S. T., Wang, D. X., and Zhang, Z. P. (2004). Mesozoic–Cenozoic tectonic relationships between the Kuqa subbasin and Tian Shan, northwest China: constraints from depositional records. *Sediment. Geol.* 172, 223–249. doi:10.1016/j.sedgeo.2004.09.002

Mao, S. Z., and Norris, G. (1988). Late cretaceous–early tertiary dinoflagellates and acritarchs from the kashi area, Tarim Basin, xinjiang province, China. *Life Sci. Contributions* 150, 1–93. doi:10.5962/bhl.title.52243

Mészáros, N., Moga, V., and Ianoliu, C. (1987). "Studying the various groups of fossil organisms of Leghia–Leghia Băi," in *The Eocene from the transylvanian basin* (Cluj-Napoca: Cluj–Napoca), 143–150.

Miller, K. G., Browning, J. V., Schmelz, W. J., Kopp, R. E., Mountain, G. S., and Wright, J. D. (2020). Cenozoic sea–level and cryospheric evolution from deep–sea geochemical and continental margin records. *Sci. Adv.* 6, eaaz1346. doi:10.1126/sciadv.aaz1346

Mount, J. (1985). Mixed siliciclastic and carbonate sediments: a proposed first–order textural and compositional classification. *Sedimentology* 32, 435–442. doi:10.1111/j.1365-3091.1985.tb00522.x

Murray, J. W. (1991). *Ecology and palaeoecology of benthic foraminifera*. Harlow, Essex, UK: Longman Scientific and Technical.

Murray, J. W. (2006). *Ecology and applications of benthic foraminifera*. Cambridge, United Kingdom: Cambridge University Press.

Pan, H., Yang, S., and Sun, L. (1991). *Late cretaceouse early tertiary gastropods, echinoids and brachiopods from western Tarim Basin, south xinjiang, China (in Chinese)*. Beijing: Science Press, 1–150.

Purser, B. H. (1973). *The Persian gulf: holocene carbonate sedimentation and diagenesis in a shallow epicontinental sea*. Berlin, Heidelberg, New York: Springer-Verlag, 1–471.

Rusu, A., Brotea, D., and Melinte, M. C. (2004). Biostratigraphy of the bartonian deposits from gilău area (NW transylvania, Romania). *Acta Palaeontol. Romaniae* 4, 441–454.

Salahi, A., and Vahidinia, M. (2011). Systematic description, paleoecology and paleobiogeography of khangiran formation oysters bivalves, in the chehelkaman synclinal, east of kopet–dagh basin. *Sci. Semiannu. J. Sediment. Facies* 4, 54–63.

Scholle, P. A., Bebout, D. G., and Moore, C. H. (1983). *Carbonate depositional environments: AAPG Memoir 33*. Tulsa, Oklahoma, United States: AAPG.

Scholle, P. A., and Ulmer–Scholle, D. S. (2003). A color guide to the petrography of carbonate rocks: grains, textures, porosity, diagenesis. *AAPG Mem.* 77.

Schweizer, M. (2006). *Evolution and molecular phylogeny of Cibicides and uvigerina (rotaliida, foraminifera)*. Ph. D. Thesis. Netherlands: Geologica Ultraiectina, 1–261.

Sobel, E. R. (1999). Basin analysis of the Jurassic-Lower Cretaceous southwest Tarim basin, northwest China. *Geol. Soc. Am. Bull.* 111, 709–724. doi:10.1130/0016-7606(1999)111<0709:BAOTJL>2.3.CO;2

Stenzel, H. B. (1971). Treatise on invertebrate Paleontology, Part N, Bivalvia. *Oysters* 3, 953–1224.

Sun, J. M., and Jiang, M. S. (2013). Eocene seawater retreat from the southwest Tarim Basin and implications for early Cenozoic tectonic evolution in the Pamir Plateau. *Tectonophysics* 588, 27–38. doi:10.1016/j.tecto.2012.11.031

Tang, T. F., Xue, Y. S., and Yu, C. L. (1992). *Characteristics and sedimentary environments of the late cretaceous to early tertiary marine strata in the western Tarim, China (in Chinese)*. Beijing: Science Press, 1–138.

Tang, T. F., Yang, H. R., Lan, X., Yu, C. L., Xue, Y. S., Zhang, Y. Y., et al. (1989). *Marine late cretaceous and early tertiary stratigraphy petroleum geology in western Tarim Basin, China (in Chinese)*. Beijing: Science Press, 1–141.

Thomas, E. (1998). "The biogeography of the late Paleocene benthic foraminiferal extinction," in *Late Paleocene–early Eocene biotic and climatic events in the marine and terrestrial records*. Editors M. P. Aubry, S. Lucas, and W. A. Berggren (New York: Columbia University Press), 214–243.

Tjalsma, R. C., and Lohmann, G. P. (1983). Paleocene–Eocene bathyal and abyssal benthic foraminifera from the Atlantic Ocean. *Micropaleontology* 4, 1–90.

Tosquella, J., Martín-Martín, M., Guerrera, F., Serrano, F., and Tramontana, M. (2022). The Eocene carbonate platform of the central-western malaguides (internal betic zone, S Spain) and its meaning for the cenozoic paleogeography of the westermost Tethys. *Palaeogeogr. Palaeoclimatol. Palaeoecol.* 589, 110840. doi:10.1016/j.palaeo.2022.110840

Tucker, M. E., and Wright, V. P. (2009). *Carbonate sedimentology*. Hoboken, New Jersey, United States: John Wiley and Sons, 1–498.

Van der Zwaan, G. J., Jorissen, F. J., and De Stigter, H. C. (1990). The depth dependency of planktonic/benthic foraminiferal ratios: constraints and applications. *Mar. Geol.* 95, 1–16. doi:10.1016/0025-3227(90)90016-D

Van Morkhoven, F. P. C. M., Berggren, W. T., Edwards, A., Morkhoven, F., Berggren, W. A., and Edwards, A. S. (1986). Cenozoic cosmopolitan deep–water benthic foraminifera. *Pau Elf-Aquitaine*.

Wang, X., Sun, D. H., Chen, F. H., Wang, F., Li, B. F., Popov, S. V., et al. (2014). Cenozoic paleo–environmental evolution of the Pamir–Tien Shan convergence zone. *J. Asian Earth Sci.* 80, 84–100. doi:10.1016/j.jseaes.2013.10.027

Wang, X. J., Xi, D. P., Mattioli, E., Wang, G. N., and Wan, X. Q. (2023). Middle Paleocene–early Eocene inter–regional correlations and palaeoclimatic changes in eastern Tethys Sea: calcareous nannofossil evidence for Paleocene–Eocene Thermal Maximum (PETM) and sea–level change from the western Tarim Basin, NW China. *Palaeogeogr. Palaeoclimatol. Palaeoecol.* 626, 111672. doi:10.1016/j.palaeo.2023.111672

Wang, X. J., Xi, D. P., Watkins, D. K., Self–Trail, J. M., Tang, Z. H., Cao, W. X., et al. (2022). Regression of the Tethys sea (central Asia) during middle to late Eocene: evidence from calcareous nannofossils of western Tarim Basin, NW China. *Mar. Micropaleontol.* 171, 102085. doi:10.1016/j.marmicro.2022.102085

Wei, J. M. (1982). Intercontinental distribution of marine territorial bivalve fossils from the Western Tarim Basin and sea (in Chinese). *Xinjiang Pet. Geol.* 4, 25–34.

Widmark, J. G. V., and Speijer, R. P. (1997). Benthic foraminiferal ecomarker species of the terminal Cretaceous (late Maastrichtian) deep–sea Tethys. *Mar. Micropaleontol.* 31, 135–155. doi:10.1016/S0377-8398(97)00008-X

Wu, S. Z. (1991). Bivalve assemblages of Paleogene at southwestern margin of Tarim Basin (in Chinese). *Xinjiang Geol.* 9, 239–248.

Xi, D. P., Cao, W. X., Cheng, Y., Jiang, T., Jia, J. Z., Li, Y. H., et al. (2016). Late Cretaceous biostratigraphy and sea–level change in the southwest Tarim Basin. *Palaeogeogr. Palaeoclimatol. Palaeoecol.* 441, 516–527. doi:10.1016/j.palaeo.2015.09.045

Xi, D. P., Tang, Z. H., Wang, X. J., Qin, Z. H., Cao, W. X., Jiang, T., et al. (2020). Cretaceous–Paleogene marine stratigraphy framework and its records of significant geologic events in the western Tarim Basin (in Chinese). *Earth Sci. Front.* 27, 165–198.

Yang, H. J., Shen, J. W., Zhang, L. J., Li, M., Huang, Z. B., and Wang, Y. (2012). Serpulids and their paleoecology of the Paleogene Kalatar Formation in southwest Tarim basin of China. *Sci. China Earth Sci.* 55, 1087–1100. doi:10.1007/s11430-012-4415-2

Yang, H. R., Jiang, X. T., and Lin, S. P. (1995). *Late cretaceous–early tertiary ostracod fauna from western Tarim Basin*, 1–173.

Yin, A., Rumelhart, P. E., Butler, R., Cowgill, E., Harrison, T. M., Foster, D. A., et al. (2002). Tectonic history of the Altyn Tagh fault system in northern Tibet inferred from Cenozoic sedimentation. *Geol. Soc. Am. Bull.* 114, 1257–1295. doi:10.1130/0016-7606(2002)114<1257:THOTAT>2.0.CO;2

Zhang, J. Y., Xing, F. C., Wout, K. M., Zhang, C., Wei, W., Chen, L., et al. (2022). Palaeogeographic reconstructions of the eocene–oligocene Tarim Basin (NW China): sedimentary response to late Eocene sea retreat. *Palaeogeogr. Palaeoclimatol. Palaeoecol.* 587, 110796. doi:10.1016/j.palaeo.2021.110796

Zhang, S. J., Hu, X. M., and Garzanti, E. (2019). Paleocene initial indentation and early growth of the Pamir as recorded in the western Tarim Basin. *Tectonophysics* 772, 228207. doi:10.1016/j.tecto.2019.228207

Zhang, S. J., Hu, X. M., Han, Z., Li, J., and Garzanti, E. (2018). Climatic and tectonic controls on Cretaceous–Palaeogene sea–level changes recorded in the Tarim epicontinental sea. *Palaeogeogr. Palaeoclimatol. Palaeoecol.* 501, 92–110. doi:10.1016/j.palaeo.2018.04.008

Zhong, S. L. (1992). *Calcareous nannofossils (coccolithophores) from the upper cretaceous and lower tertiary in the western Tarim Basin, south xinjiang, China (in Chinese)*. Beijing: Science Press, 1–121.

Zhou, Z. Y., and Chen, P. J. (1992). *Biostratigraphy and geological evolution of Tarim*. China: Science Press, 1–399.

Zhou, Z. Y., Zhao, Z. X., Hu, Z. X., Chen, P. J., Zhang, S. B., and Yong, T. S. (2001). *Strata in Tarim Basin (in Chinese)*. Beijing: Science Press, 1–359.

Zwaan, G. J., Duijnstee, I. A. P., Dulk, D. M., Ernst, S. R., Jannink, N. T., and Kouwenhoven, T. J. (1999). Benthic foraminifers: proxies or problems? A review of paleoecological concepts. *Earth Sci. Rev.* 46, 213–236. doi:10.1016/S0012-8252(99)00011-2